Physics of the seasonal sea ice zone

Lettie A. Roach,[1,2] Madison M. Smith,[3], Agnieszka Herman[4] and Damien Ringeisen[1,2]

[1]Center for Climate Systems Research, Columbia University, New York, NY, USA; email: l.roach@columbia.edu
[2]NASA Goddard Institute for Space Studies, New York, NY, USA
[3]Woods Hole Oceanographic Institution, Woods Hole, MA, USA
[4]Institute of Oceanology, Polish Academy of Sciences, Sopot, Poland

Xxxx. Xxx. Xxx. Xxx. YYYY. AA:1–26

https://doi.org/10.1146/((please add article doi))

Keywords

sea ice; polar oceans; Arctic; Antarctic; climate

Abstract

The seasonal sea ice zone encompasses the region between the winter maximum and summer minimum sea ice extent. In both the Arctic and Antarctic, the majority of the ice cover can now be classified as seasonal. Here we review the sea ice physics that governs evolution of seasonal sea ice in the Arctic and Antarctic, spanning sea ice melt, growth and dynamics and including interactions with ocean surface waves, as well as other coupled processes. The advent of coupled wave-ice modeling and discrete element modeling, together with improved and expanded satellite observations and field campaigns, have yielded advances in process understanding. Many topics remain in need of further investigation, including rheologies appropriate for seasonal sea ice, wave-induced sea ice fracture, welding for sea ice freeze-up, and the distribution of snow on seasonal sea ice. Future research should aim to redress biases (such as disparities in focus between the Arctic and Antarctic, or summer and winter processes) and connect observations to modeling across spatial scales.

Contents

Seasonal sea ice zone: The extent of sea ice between the seasonal minimum and seasonal maximum extent limits.

Sea ice extent: The surface area of the ocean where the sea ice concentration exceeds 15 %

1. INTRODUCTION

The sea ice cover at both poles is now largely seasonal (Fig. 1). According to satellite observations, the majority of Antarctic sea ice cover retreats back to the continent each year, to a degree that has been largely consistent since continuous satellite observations began in the late 1970s (Fig. 2). On average, 15 % of the maximum sea ice extent remains throughout the summer minimum, such that 85 % of the Antarctic sea ice extent is seasonal. In contrast, a clear trend is evident in the Arctic: 52 % of the sea ice was seasonal in the 1980s, increasing to 67 % in the 2010s.

The seasonal advance and retreat of sea ice has enormous implications for weather and climate, ocean circulation, ecosystems and—in the Arctic—local communities. As sea ice retreats seasonally, it exposes darker ocean waters, lowering global albedo and enhancing the absorption of solar radiation. The newly uncovered ocean has a much greater capacity to store heat than sea ice, slowing the seasonal ocean cooling rate in autumn. Sea ice melt freshens the ocean while sea ice growth increases its salinity, impacting ocean circulation. Sea ice provides a habitat for ice algae, a fundamental part of the food web, to remain suspended in the upper layers of the ocean and attract zooplankton. Higher trophic level species such as polar bears and seals rely on the ice as a physical platform, and sea ice loss has dramatically impacted these species as well as the people for whom hunting and fishing have been a traditional way of life.

Recent reviews of sea ice have largely focused on interactions between sea ice and ocean surface waves (Thomson 2022, Horvat 2022, Dumont 2022, Shen 2022), and long-term trends in sea ice (Maksym 2019). Here we review the sea ice physics that governs evolution of the seasonal ice cover in both the Arctic and Antarctic. Our review includes a broad set of processes encompassing sea ice melt, growth and dynamics, including interactions with ocean surface waves as well as other coupled processes. We aim to provide a comprehensive view of the sea ice life cycle and to highlight processes that remain under-explored. While the physical processes involved in shaping the evolution of sea ice are intrinsically coupled with processes in the lower atmosphere and the upper ocean, this review takes a sea ice-centric perspective.

This review is structured as follows. We discuss representations of the sea ice state in Sec. 2 and the simple physics governing the seasonal cycle in Sec. 3. In Sec. 4, we review

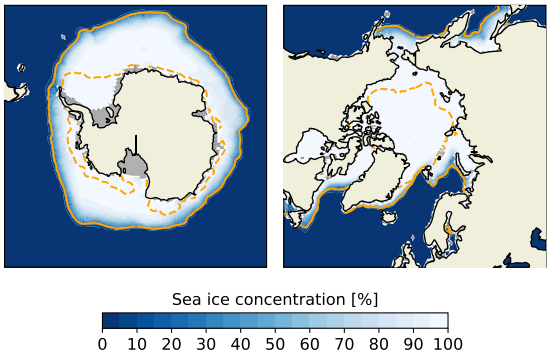

Figure 1: 2004-2023 mean sea ice concentration from NSIDC CDR version 4 observations (Meier et al. 2021), in the months of winter maximum: (a) September in the Antarctic and (b) March in the Arctic. Orange contours show the 15% sea ice concentration contour in that month and (dashed) the month of summer minimum, such that the area between represents the typical seasonal sea ice extent in the last two decades.

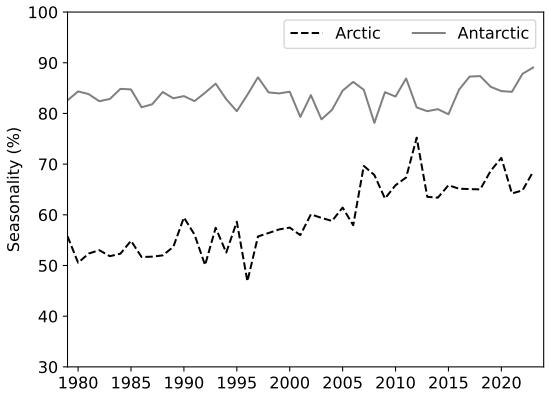

Figure 2: Sea ice seasonality based on sea ice extent (SIE) from NSIDC CDR version 4 observations (Meier et al. 2021), defined as $100\% \times \left(1 - \frac{\min(\mathrm{SIE})}{\max(\mathrm{SIE})}\right)$.

current understanding of the sea ice physics relevant for seasonal sea ice, including growth, dynamics and melt, and in Sec. 5 we highlight areas that require further investigation.

2. SEA ICE STATE

Seasonal sea ice is a complex, multi-component material. Depending on local conditions and its history, a given volume of sea ice (blue rectangle in Fig. 3) contains a large number of individual, discrete objects, from single frazil crystals and their agglomerates up to very large floes (with length scales on the order of kilometers). The ith of these components has a unique set of N relevant properties, $p_i^1, p_i^1, \ldots, p_i^N$ (density, surface and bottom roughness,

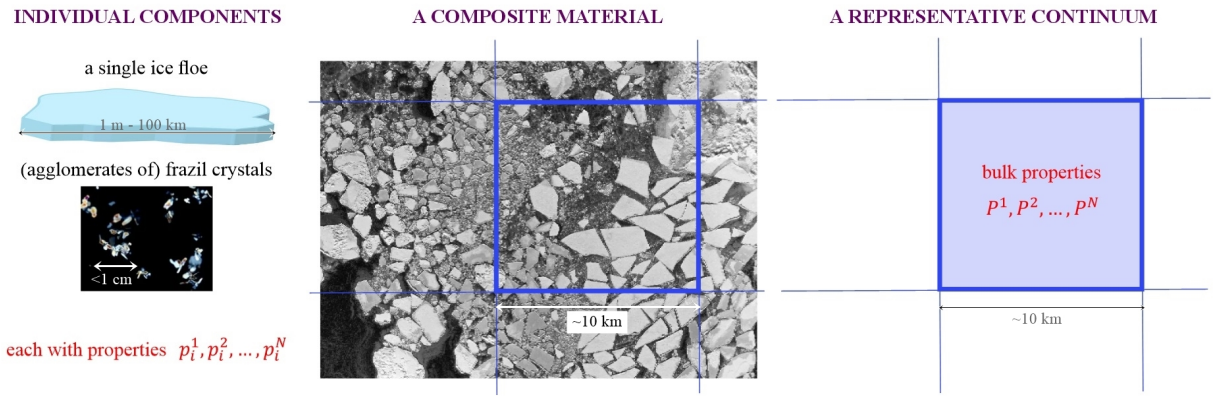

Figure 3: Sea ice: from individual components (floes, frazil crystals, etc.) to a complex mixture and its continuum representation used in models (see section 2 for details). Image in the middle: seasonal sea ice in the northern Baltic Sea on 19 March 2020 (drone photo by David Brus).

thickness, diameter, elastic modulus, and so on). Even over a single floe, properties such as salinity, thickness, snow cover, and the presence of ridges vary. Together, the components form a mixture with bulk properties $P^1, P^2, \ldots, P^N$ that depend on the properties of individual components in a nontrivial way. The challenge for theoretical and numerical modeling of sea ice is to find a continuum representation of this complex mixture, capturing its behavior in response to forcing from the ocean, atmosphere and surrounding ice, as has traditionally been easier to incorporate in earth system models.

Early climate models reduced the heterogeneity of real-world sea ice cover to very simple representations, for example temperature-dependent formulations of albedo to implicitly represent sea ice, fractional sea ice concentration, or grid cell mean thickness. These simple approaches were sufficient to develop understanding of the sea ice albedo feedback and polar amplification (e.g., Budyko 1969). Further detail can be gained by considering the ice thickness distribution (Thorndike et al. 1975), a probability distribution of sea ice thickness within a given area. Although seasonal sea ice is typically thinner than multi-year ice, and the thickness distribution in the Arctic has shifted over the past 30 years, ice thickness can still range from 0 to 4+ meters (e.g., Sumata et al. 2023), a variation that yields enormous differences in heat transfer and dynamical properties.

Another representation of sea ice is the floe size distribution (FSD), a probability function that characterizes the variability in the horizontal size of sea ice floes. Floe sizes can vary over an extremely broad range, from centimeters to hundreds of kilometers (Rothrock & Thorndike 1984). The ice thickness and floe size distributions can be combined into a joint probability distribution (Horvat & Tziperman 2015). However, in regions where floes cannot be clearly identified or delineated, the FSD is challenging to define. This is especially true for pack ice, but can also be the case in seasonal ice cover, particularly for young ice types. Even when floes are clearly separated in satellite imagery, identifying floes and determining their size distribution is not easy: this has strongly limited observations, although new methods are leading to improvements (e.g., Buckley et al. 2024). The floe size number density from satellite or aerial imagery in the SIZ is often characterized by a

power law, although the exponent and goodness-of-fit vary (e.g. Toyota et al. 2011, Stern et al. 2018, Horvat et al. 2019, Buckley et al. 2024).

In contrast to the continuum representations described above, a discrete element representation of sea ice considers large numbers of colliding bonded elements of specified shapes and contact laws as individuals floes, which may or may not be able to change shape (e.g., Manucharyan & Montemuro 2022). Another discrete representation of sea ice is the frequency of ice type (e.g., first-year ice, grease ice, pancake ice, see Sec. 4.1). Ship-based campaigns often quantify sea ice types via the Antarctic Sea Ice Processes and Climate (ASPeCt) protocol into ice type, topography, thickness and snow cover categories. It is possible to compare these against models (e.g., Timmermann 2004), but earth system models typically do not consider different types of sea ice, except occasionally a separate grease ice category (e.g., Smedsrud & Martin 2015). The occurrence of different ice types is not necessarily related to a given area's ice concentration or thickness, and multiple ice types can occur within areas of a few meters, with different impacts for dynamics and heat fluxes (see Sec. 4).

More broadly, hemispheric or regional variations in sea ice can be quantified using sea ice area, extent or volume. Recent years have seen an increased scientific focus on the 'marginal ice zone' (MIZ), whose extent can vary enormously depending on the definition chosen. The MIZ is defined by the World Meteorological Organization (WMO) as 'the region of an ice cover which is affected by waves and swell penetrating into the ice from the open ocean,' without a quantitative definition. Based on quantities that are well-observed by satellite, a quantitative definition of the MIZ is 'the area of the ice-covered ocean that is adjacent to the open ocean and where the ice concentration is less than 80% and more than 15%;' however, this does not necessarily nor typically correspond to the area of sea ice affected by waves. One could define the MIZ based on ocean surface wave properties (for example, Sutherland & Dumont 2018, using the wave radiation stress) or FSD properties; both would more closely correspond with the WMO definition, but are difficult to observe. A recently proposed definition for the Antarctic based on sea ice variability could be a new path forward (Vichi 2022). In general, which of these quantities is most useful depends on the science question at hand. Here, to avoid ambiguity, we focus on the seasonal sea ice zone (SIZ) rather than the MIZ. The SIZ is the region between the winter maximum and summer minimum sea ice extent. As sea ice extent is defined by the 15% sea ice concentration contour, the SIZ has low observational uncertainty and is straightforward to quantify. The region is affected by a broad range of physics, including but not limited to those associated with ocean surface waves. It can also be thought of as the region that has been, and will be, an MIZ over the course of the year.

3. A FIRST-ORDER VIEW: SIMPLE PHYSICS

Seasonal changes in sea ice extent and thickness are, to first order, driven by the seasonal response to solar and longwave radiative forcing. This can be described using a simple set of equations following, for example, Wagner & Eisenman (2015).

Consider a diffusive energy-balance model that simulates the evolution of the zonal-mean climate in an aquaplanet, neglecting the specific heat capacity of sea ice and the atmospheric column. The state variable is the enthalpy of the surface layer and the atmospheric column,

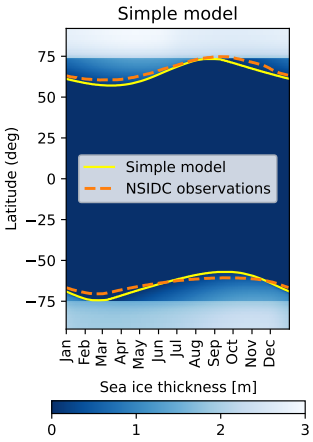

Figure 4: Zonal-mean seasonal cycle of sea ice thickness in the simple model described in Sec. 3. The seasonal evolution of the ice edge defined by $\mathcal{E} = 0$ from the model is shown in yellow and the 15 % sea ice concentration contour for the 1979-1998 climatology in NSIDC satellite observations is shown in orange dashed.

Enthalpy $\mathcal{E}$: a state function of a thermodynamic system, defined as a sum of its internal energy and a product of its volume and pressure

Planetary coalbedo a: the fraction of incoming solar radiation absorbed by the Earth. In the simple model described here, it is given by a_i in the case $\mathcal{E} < 0$ (sea ice) or a_w in the case $\mathcal{E} \geq 0$ (open water), where $a_w = a_0 - a_2 \sin^2\theta$ with θ the latitude and a_i, a_0, and a_2 constants.

$\mathcal{E}$, which is defined as

$$\mathcal{E} \equiv \begin{cases} -L_f\, h, & \mathcal{E} < 0 \text{ (sea ice)} \\ c_w\,(T - T_f), & \mathcal{E} \geq 0 \text{ (open water)} \end{cases}, \tag{1.}$$

where L_f is the latent heat of fusion, h is sea ice thickness, c_w is the heat capacity of the ocean mixed layer, T is the surface temperature, and T_f is the freezing point. The enthalpy, $\mathcal{E}$, evolves due to the net balance of top-of-atmosphere insolation S scaled by planetary coalbedo a, outgoing longwave radiation which is approximated as $c_1 + c_2\,(T - T_f)$ with c_1 and c_2 constants, meridional heat transport parameterized as diffusion $D\,\nabla^2 T$, and a constant heat input from the ocean F_b, such that

$$\frac{\partial \mathcal{E}}{\partial t} = a\,S - [c_1 + c_2\,(T - T_f)] + D\,\nabla^2 T + F_b. \tag{2.}$$

When $\mathcal{E} < 0$, Eq. (2) describes the evolution of sea ice thickness h. In this case, the surface temperature that would balance the surface atmospheric energy flux with the vertical heat flux through ice, T_0, is given by,

$$k\,\frac{T_f - T_0}{h} = -a\,S + [c_1 + c_2\,(T - T_f)] - D\,\nabla^2 T, \tag{3.}$$

where k is the thermal conductivity of the ice and assuming a linear temperature profile in the ice. The surface temperature is given by,

$$T \equiv \begin{cases} T_f + \mathcal{E}/c_w, & \mathcal{E} \geq 0 \text{ (open water)} \\ T_f, & \mathcal{E} < 0, T_0 > T_f \text{ (melting ice)} \\ T_0, & \mathcal{E} < 0, T_0 < T_f \text{ (subfreezing ice)} \end{cases}. \tag{4.}$$

This model is integrated with c_1 tuned to match the observed annual-mean zonal-mean ice edge latitude and other parameters as described in Roach et al. (2022). Such a simple model can qualitatively capture the observed seasonal evolution of the zonal-mean ice edge latitude in the Arctic and Antarctic (Fig. 4). However, this representation is an enormous simplification of the extraordinarily heterogeneous real-world sea ice cover as well as the complex air-ice-ocean dynamical and thermodynamical processes that shape it.

4. A MORE COMPREHENSIVE VIEW: THE SEA ICE LIFE CYCLE

In this section, we review the sea ice physics that govern evolution of the seasonal ice cover in both the Arctic and Antarctic, including sea ice growth, melt and dynamics. The growth and melt phases can be considered as a thermodynamic 'life cycle' (Fig. 5) that occurs each year, with the caveat that some processes may occur continuously in localized areas, such as the outer margins of the sea ice zone. In contrast, dynamical processes may generally occur at any time during the year throughout the ice cover. Their implications for sea ice mass balance and atmosphere-ocean interactions are governed by their timing within the seasonal cycle.

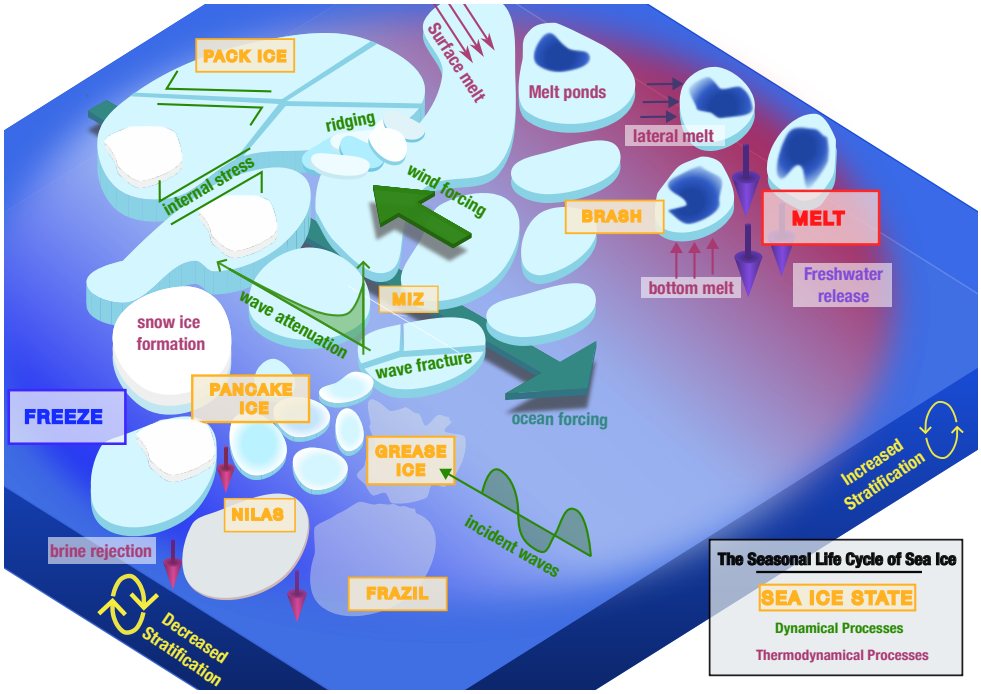

Figure 5: Growth, melt and dynamical processes relevant for seasonal sea ice.

4.1. Sea ice growth

Sea ice growth occurs due to the unique properties of seawater and its interactions with the overlying atmosphere and underlying ocean. The mode of sea ice growth influences sea ice dynamics and ice-ocean-atmosphere heat transfer, playing a major role in SIZ evolution, especially during the ice advance period.

To first order, sea ice forms when the top layer of the ocean reaches the freezing point. This occurs in high latitudes where the ocean is characterized by a permanent halocline that separates a fresher upper ocean layer from a warm saltier layer at depth. As seawater is cooled from above, the vertical difference in salinity limits mixing of warmer water from below, allowing the formation of sea ice (Roquet et al. 2022). The presence of salt ions

lowers the freezing point for typical seawater to approximately -1.8 °C. Once the upper layer is cooled below its freezing point, sea ice can begin to form on the surface of the ocean. The highest rates of new ice production occur in latent heat polynyas near the coast, in both the Arctic and Antarctic (Nakata et al. 2021).

The properties of the sea ice that forms depend strongly on the presence and strength of ocean turbulence. This turbulence might be associated with wind shear, ocean surface waves and/or buoyancy-driven convection (Herman et al. 2020). If the ocean surface is turbulent, freezing can occur throughout the ocean surface layer, whereas in quiescent conditions, freezing only occurs at the surface.

Initial seed crystals in the surface ocean originate from the sublimation of water vapor in a cold atmosphere or from the freezing of water droplets produced by breaking ocean surface waves (Daly 1994). The initial crystals that form are disk-shaped and typically around 0.5 mm in size (Schneck et al. 2019). If the water temperature is below freezing, crystals grow at a rate that depends on the rate at which latent heat is transported away from the crystal, which may be higher than previously thought (Rees Jones & Wells 2015). When crystals collide in the presence of turbulence, fragmented pieces become the nuclei for new crystals, a secondary nucleation process that represents a positive feedback (Clark & Doering 2009) and can be modeled as collisions between crystals belonging to discrete size classes (Holland & Feltham 2005, Heorton et al. 2017). Besides crystal growth and nucleation, the rate of gravitational removal is also an important control on frazil ice formation (Rees Jones & Wells 2018).

The dynamics of the frazil crystal and seawater mixture are largely driven by the buoyant rising of frazil crystals (Morse & Richard 2009) and turbulent diffusion. Frazil crystals precipitate into the boundary layer at the air-ocean interface, a viscous sublayer where viscous stresses dominate and the flow velocity decreases to zero at the interface. There, they can be herded by winds and/or waves into a slushy mix of seawater and frazil, termed 'grease ice.' The grease ice accumulation rate depends on wind speed, ocean currents, drag and resistance forces (Smedsrud 2011, Smedsrud & Martin 2015). As heat loss to the atmosphere continues, the fraction of solid ice increases. Brine is trapped between growing crystals as it forms, so new sea ice can have salt content as much as 50% that of seawater (Wakatsuchi & Ono 1983).

If the ocean surface is turbulent, as the grease ice consolidates, wave-induced collisions and dilation form it into near-circular floes with upturned edges, termed 'pancakes.' The frazil-to-pancake transition takes place on a timescale of around 24 hours (Doble 2009). The newly-forming sea ice modifies the ocean surface wave field, damping wave energy, particularly at high frequencies, see Sec. 4.2.2. Pancake floes mostly follow wave motion (Smith & Thomson 2020). Their horizontal sizes are controlled by the properties of the ocean surface waves, and are rarely smaller than 2 cm (Shen et al. 2001, Shen & Sankaran 2004). The maximum pancake diameter can be limited either by the tensile stress (where differential wave force creates 'stretching' of the surface between floes) or bending stress (where vertical tensile force creates bending force on floes), according to theory developed for a monochromatic wave (Shen et al. 2001, Roach et al. 2018b).

At diameters beyond one quarter of the wavelength, there is no longer a wave control on pancake diameter, and pancakes can grow indefinitely. Pancakes can grow in diameter via lateral growth as well as freezing together with neighbors to form composites and by incorporating interstitial frazil crystals, resulting in sheets of consolidated or 'welded' pancakes. The rate of welding depends on the distribution of pancakes across the domain, and other

Polynya: large, persistent regions of open water and thin ice that occur within much thicker pack ice, typically on the order of 100 km in length. They can be formed due to upwelling of warm water (sensible heat polynya) or due to the action of katabatic winds (latent heat polynya). In the latter case, sea ice is advected away by winds, allowing high rates of new sea ice production.

Frazil ice: Millimeter-scale needle or plate-like crystals of sea ice.

Grease ice: Coagulation of frazil ice crystals into a soupy layer on the surface, which has a 'grease-like' or matte appearance.

Pancake ice: Roughly circular pieces of ice with raised edges due to the collisions with one another. Typically tens of cenimeters to meters in diameter.

Nilas: A thin (< 10 cm) elastic layer of ice which bends easily with waves and, under pressure, can raft in a pattern of interlocking 'fingers' (finger rafting).

Congelation growth: A bottom-freezing process that occurs via the downward growth of the ice crystals into the water. Congelation ice has a distinctive columnar crystal texture.

thermodynamic and dynamic factors (Roach et al. 2018b). The frequency and severity of pancake ice floe collisions in an active wave field increase with the wave period (Marquart et al. 2023). During collisions, pancakes may raft on top of one another; rafted pancake ice thickness strongly increases with wind speed (Dolatshah et al. 2019). These different thermodynamic and dynamic processes result in a multi-regime pancake FSD (Alberello et al. 2019) and differences in pancake ice properties between the Arctic and the Antarctic (Nose et al. 2020), with the latter generally subject to stronger winds and waves.

On the other hand, if the ocean surface is calm rather than turbulent, frazil crystals may freeze together into 'nilas': thin, semi-transparent ice sheets. Nilas is typically up to 10 cm thick and appears dark gray, therefore having a smaller impact on albedo than pancake ice. The volume of ice produced via pancake ice formation can be twice as high as that produced via nilas formation, as pancake ice formation allows increased heat flux from the ocean to the atmosphere to occur during freeze-up (Doble 2009, Naumann et al. 2012).

Both pancakes and nilas subsequently thicken. The increase in thickness typically occurs via congelation growth, the downward growth of ice crystals into the water. The rate of downward congelation growth is determined by the net balance of fluxes at the ice–ocean interface and is also modestly impacted by salt transport between the two media (Wells et al. 2019). Brine loss from sea ice occurs via temperature-dependent brine pocket migration, brine expulsion, and, most importantly, by gravity drainage via a network of cells and channels. Brine loss can enhance sea ice formation, as well as being a key driver of ocean circulation through the creation of dense water. In supercooled water, such as near Antarctic ice shelves, sea ice can also thicken due to formation of additional frazil crystals at the underside of the existing ice (Gough et al. 2012).

An additional mode of sea ice growth is snow-ice formation. If the ratio of snow accumulation (from precipitation or snow redistribution) on top of sea ice is sufficiently large compared to the ice thickness as to push the ice surface below sea level, seawater can permeate the snow on sea ice, which can then freeze into ice. Snow-ice formation can also occur when high ocean heat fluxes lead to basal melt, sea ice thinning and flooding of the overlying snow. Snow-ice formation rates may exceed congelation growth rates regionally (Zhaka et al. 2023). Snow-ice formation is more common in the Antarctic, which has high precipitation rates and thin sea ice that can more easily be depressed than in the Arctic, and may represent around a quarter of total sea ice formation there (Jeffries et al. 2001).

4.2. Sea ice dynamics

Throughout its life cycle, sea ice is subjected to a range of dynamic forcings, including winds, ocean currents, waves and internal stresses. These forcings govern the drift of sea ice, which helps determine its extent and concentration, as well as the mechanical redistribution of sea ice via rafting and ridging, which helps determine sea ice thickness (e.g. Worby et al. 2008).

Due to its low density, sea ice is positively buoyant. Apart from frazil crystals (Sec. 4.1), which can move vertically in the water column depending the balance between gravity, buoyancy and drag that depends nonlinearly on the size, shape, and orientation of crystals (e.g., McFarlane et al. 2014), all other forms of ice remain at the surface and, most of the time, stay in hydrostatic equilibrium Motion of large floes due to waves is an exception to this rule, see further Sec. 4.2.2. Thus, in most situations, it is justified to analyze the motion and deformation of sea ice in two horizontal dimensions.

Forces acting on ice floes can be divided into two groups: those proportional to the ice mass (body forces, e.g., the along-surface component of the gravitational force in the case of nonzero gradients of sea surface height, or the Coriolis force), and those proportional to the surface area on which the force is acting (surface forces, including stresses from the ocean, atmosphere and surrounding ice). The surface stresses can be further divided into tangential and normal wind stresses (related to skin and form drag, respectively) acting on the parts of ice floes protruding from the water; tangential and normal oceanic stresses acting on submerged parts of ice floes; and internal stress, related to collisions/friction between floes (contact stress) and to turbulent-like motion of floes (kinetic stress). The common feature of all three stress sources is their dependence on the relative velocity between ice and air, water and surrounding floes, respectively. Due to the nonlinear nature of these relationships, the net stresses analyzed at sufficiently large spatial and temporal scales depend not only on the mean wind, current and ice velocities, but also on their high-frequency fluctuations: wind gustiness, turbulent ocean eddies, wave motion, and floe–floe collisions (see, e.g., Feltham 2005, Andreas et al. 2010, Manucharyan & Thompson 2017, Gupta & Thompson 2022, Brenner et al. 2023, Gupta et al. 2024, and references therein). On hourly timescales, an additional source of stress are tidal currents and inertial oscillations (e.g., Womack et al. 2024).

Skin drag: drag caused by friction between a fluid and object moving through it, influenced by object's surface roughness and fluid viscosity

Form drag: drag caused by pressure difference between front and rear surface of a moving object, influenced by the object's shape

Contrary to a dense ice pack, in which the primary force balance is between the average wind, ocean current and internal ice stress, in seasonal ice the net effects of fluctuations of the forcing and the ice itself are significant. We are only just beginning to understand and appreciate the role of these processes. The following subsections present current knowledge on (1) horizontal surface stresses from wind and ocean, (2) wave-induced processes, including vertical and horizontal stresses, and the fracturing of ice floes, and (3) internal stresses and sea ice rheology.

4.2.1. Wind and ocean stresses. The primary driver of sea ice dynamics in the SIZ is wind stress, while ocean currents typically act as a drag on sea ice motion. The stresses exerted on sea ice by wind and currents depend on ice concentration (A) and morphology, i.e., the sizes of and distances between roughness elements at the upper and lower surface of the ice. Depending on ice type and state, the roughness elements are floe edges, ridges, rafted pancakes, snow formations, sub-ice frazil crystals etc. All these features affect the bulk drag coefficients of the top and bottom surface of the ice, $C_{\mathrm{d,ai}}$ and $C_{\mathrm{d,oi}}$, respectively. Due to the large variability of surface properties, both $C_{\mathrm{d,ai}}$ and $C_{\mathrm{d,oi}}$ vary strongly, from well below 10^{-3} for grease ice up to over 10^{-2} for deformed ice (Brenner et al. 2021, and references therein). Importantly, in the ice pack the bulk ice–ocean and ice–atmosphere drags are highest in the range of middle ice concentrations: if A is very low (below 0.2–0.3), the bulk drag is low due to the roughness of open water being lower than that of the ice; if the floes are densely packed ($A \sim 1$), the neighboring roughness elements are less effective due to a sheltering effect (e.g., Lu et al. 2011, Tsamados et al. 2014).

For individual ice floes, the skin drag acting on their top/bottom surface is proportional to their surface area, and the form drag acting on their edges is proportional to their diameter. The proportionality of surface forcing leads to a size-dependent response of floes to the forcing and is one of the mechanisms of floe clustering (Herman 2011, 2012), with patches of densely packed floes even when $A \ll 1$. Generally however, as long as A remains below $\sim$0.8 internal stress in the ice (see further Sec. 4.2.3) remains low and the ice is in free drift, moving at approximately 2–4% of the wind speed (Wagner et al. 2022). In the

Antarctic MIZ, however, free drift is observed even at $A \sim 1$ (Womack et al. 2022). Strong influence of ice type and morphology on the drag coefficients leads to a pronounced seasonal cycle of ice–ocean and ice–atmosphere stresses observed in the Arctic, with a minimum in late autumn and a maximum in late spring (e.g., Brenner et al. 2021, Mchedlishvili et al. 2023). Relatively simple parametrizations of drag in which the drag coefficient is linearly proportional to the ice thickness, combined with a free-drift assumption, successfully capture seasonal variability in Arctic ice drift at large scales (Brunette et al. 2022).

Free drift: a mode of sea ice motion under equilibrium between the oceanic, atmospheric and Coriolis force, with zero internal stress.

4.2.2. Wave stresses and fracture. Ocean surface waves dynamically impact sea ice cover by influencing sea ice formation (Sec. 4.1), exerting stresses that act horizontally and vertically, and wave-induced fracture. These are coupled interactions, as sea ice in turn influences waves by attenuating wave energy. Wave–sea ice feedbacks play an important role in the evolution of the SIZ. For example, larger wave radiation stress may compact the SIZ, so that it is more resistant to other stresses; while a fractured sea ice field leads to less wave attenuation, enhanced ice melt and reduced sea ice cover. As several reviews of wave dynamics in the MIZ have recently been published (Thomson 2022, Shen 2022, Dumont 2022), we include only a brief summary here.

Swell grows in open water under wind forcing and propagates into sea ice from tens to thousands of kilometers away. Waves can also be generated locally by wind in open ocean near sea ice, or in partially ice-covered regions. Once waves enter sea ice, wave energy is attenuated with distance into the sea ice, at a rate that largely depends on sea ice concentration. The decrease of wave energy, E, as a function of frequency, f, with distance into sea ice, x, is typically modeled with an exponential decay (e.g. Thomson 2022, Squire 2018),

$$E(f,x) = E(f,0)\exp^{-\alpha(f)x}. \qquad 5.$$

The attenuation rate $\alpha(f)$ increases with the frequency of the waves, and is typically observed to be a power law in incident wave frequency $\alpha \propto f^p$ with $2 \leq p \leq 4$, meaning that high frequency waves are most rapidly attenuated. Higher order or linear attenuation rates may be more appropriate in some situations (Squire 2018, Kohout et al. 2014). The attenuation rate is also expected to depend on the state of the sea ice cover, including ice type, thickness, concentration and floe size. It can increase five-fold in the winter compared to the spring, due to changes in sea ice state (Wahlgren et al. 2023).

Waves are attenuated in sea ice by scattering or dissipation. Scattering conserves wave energy and can cause changes in wave direction, and is most relevant for floes with length scales similar to the wavelength. Dissipation is non-conservative, and is beginning to be thought of us as the more important of the two mechanisms (Thomson 2022). The main processes by which wave energy dissipation occurs are turbulence at the ice-ocean interface arising from differential velocity between sea ice and orbital wave motion (Voermans et al. 2019); fracture of sea ice floes (Ardhuin et al. 2020); and inelastic collisions between floes (Smith & Thomson 2020). In-situ observations suggest that dissipation by turbulence may be more important than floe collisions (Smith & Thomson 2020).

The dissipation of wave energy at the ice-ocean interface creates stress in the direction of the wave propagation, that is referred to as 'wave radiation stress' (WRS) and can be expressed as (Longuet-Higgins & w. Stewart 1964):

$$\tau = -\nabla \cdot \mathbf{R} = -\frac{\partial R_{ij}}{\partial x_i}\hat{\mathbf{e}}_\mathbf{j}, \qquad 6.$$

where $\mathbf{R}$ (and its components R_{ij}) is a tensor that depends on the wave amplitude, group and phase speed and orientation, and wave number spectrum. By considering that all the energy dissipated in the attenuation is transferred to the ice as momentum and that the wave is aligned on the x direction, the equation can be simplified as (Dumont 2022)

$$\tau_x = -\frac{1}{2}\rho g \frac{dE}{dx}, \tag{7.}$$

where $\frac{dE}{dx}$ is given by Eq. 5. The WRS pressure has been measured in the $[0.1, 1]$ Pa range and acts as a stabilizing factor for sea ice(Stopa et al. 2018). WRS typically acts from open ice into the sea ice cover and therefore compacts sea ice, making it more resistant to wind stress and deformation (Boutin et al. 2020). The WRS can be stronger than the wind stress in low wind conditions in the edge (~ 50 km) of the sea ice cover (Stopa et al. 2018).

Sea ice, at the floe scale, is a brittle material: it does not deform much before breaking into several pieces. Sea ice fracture events due to waves are common at large scales (Kohout et al. 2014, Prinsenberg & Peterson 2011), or even at the scale of a single ice floe (Herman et al. 2021). Different criteria governing the fracture of sea ice floes have been proposed (Dumont et al. 2011). The two main methods are based on (1) the deformation of the ice floe assuming that the floe follows exactly the sea surface height field, and fractures when a critical flexural strain limit is reached, and (2) the stress applied by the wave on the ice assuming that the ice is rigid and does not deform, and fractures when the flexural strength is reached. These two approaches can be used in combination by applying (1) to short waves and (2) to long waves (Dumont et al. 2011, Williams et al. 2013). Both are imperfect assumptions: ice can deform due to the waves and does not necessarily flex with the sea surface height field. The value for the fracture threshold based on flexural strain, $I_{br} = 0.014$, agrees well across observations and laboratory experiments (Voermans et al. 2020), as well as values found by statistical analysis in a pan-Arctic model (Boutin et al. 2018).

Wave-induced fracture can rapidly modify the sea ice FSD. Sea ice fractures preferentially into sizes close to half the incident wavelength, giving log-normal, Gaussian or modal FSDs according to detailed strain-based modeling applied to each floe (Mokus & Montiel 2022) or observations (Herman et al. 2021, Dumas-Lefebvre & Dumont 2021). Fractured sea ice exposes the edges of floes to the open ocean, and can enhance lateral melt (see Sec. 4.3) or growth.

Strain ε: nondimensional measure of relative deformation of a body, compared to its reference shape and position.

Strain rate $\dot{\varepsilon}$: time derivative of strain, measured in s^{-1}

4.2.3. Sea ice internal stresses. Sea ice internal stress is variable and poorly-understood, but plays an important role in deformation. The response of a given volume of sea ice mixture to forces from the surrounding ice is described by a rheological model: constitutive equations relating the applied stress σ_{ij} to strain ε_{ij} and/or strain rate $\dot{\varepsilon}_{ij}$, and to bulk material properties (elastic modulus, viscosity, etc.; see, e.g., Irgens 2014).

In the case of sea ice, with its wide range of sizes of crystals and/or floes, its rheological properties are closely related to the scale at which deformation is analyzed. All rheology models of sea ice assume a clear separation of scales between the characteristic size of individual floes, $\bar{d}$, and the scale L at which macroscopic deformation takes place: $\bar{d} \ll L$. Equivalently, the number of crystals/floes in the analyzed volume of ice should be sufficiently large to capture natural variability. This assumption is unproblematic in young ice types (grease ice, shuga, pancakes, small ice floes), as well as, most of the time, at scales of tens of kilometers in an ice pack, i.e., scales corresponding to typical mesh resolution of global

and regional models. In that case, the actual value of $\bar{d}$ becomes irrelevant. Accordingly, no information about floe size is used in the rheologies suitable for large-scale analysis of sea ice dynamics, including the classical viscous-plastic rheology of Hibler (1979) and its later variants (see Feltham 2008, for an overview), as well as the recently developed elasto-brittle models (Dansereau et al. 2016, Ólason et al. 2022). In Arctic-wide simulations, elasto-brittle rheology captures essential features of sea ice deformation, including many (but not all) statistical properties of localization and scale-invariance of deformation (Bouchat et al. 2022). However, for many situations in seasonal sea ice, $\bar{d}$ is, first, hard to determine, and second, comparable with L: the ice is a mixture of floes spanning a very wide range of sizes, from less than a meter to tens of kilometers, and the largest floes have sizes similar to the width of the MIZ, dimensions of a strait or channel through which ice is moving, or the sizes of ocean eddies naturally defining (and limiting) the length scale L. In that case, floe-size effects cannot be disregarded, and the ice behaves as a polydisperse granular material (Herman 2022).

The only granular rheology that has been proposed for sea ice is that of Feltham (2005), based on a series of papers from 1980s by Shen and coauthors (Shen et al. 1984, 1986, 1987). It is based on the kinetic theory of dry granular gases and thus shares important assumptions with that theory. Many of them are unrealistic when applied to sea ice. In particular, it is assumed that ice has high restitution coefficient and that ice floes, randomly distributed on the sea surface, undergo short-lived, binary collisions, but no prolonged contacts (in both cases, observations show otherwise, see Yulmetov et al. 2016, Li & Lubbad 2018, and references therein). Also, the presence of ice or water/frazil mixture between floes, influencing floes' motion between collisions and the nature of collisions themselves, is disregarded. Moreover, although collisional rheology has been useful in some applications (e.g., Rynders et al. 2022), it can be treated as an acceptable approximation of real sea ice only under a very narrow range of conditions: the ice concentration must be sufficiently low to allow individual motion of ice floes and sufficiently high to sustain collisions between neighboring floes. A much more common situation in the SIZ, especially its inner parts, is that corresponding to a dense granular flow, i.e., a state in which a typical floe undergoes several contacts with its neighbors at the same time, and many of those contacts are long-lived.

One of the most widely-used rheological models in applied research on granular materials is the so-called $\mu(I)$ rheology (Jop et al. 2006, Jop 2015). Based on simple dimensional analysis, it states that the friction coefficient μ of a granular material is a function of only one, nondimensional parameter, namely the inertial number I, defined as: $I = \dot{\varepsilon} d/\sqrt{p/\rho}$, where p and ρ denote pressure and density, respectively, and d is a length scale associated with microscopic rearrangements of grains. Although the original model has been formulated for two-dimensional, dry materials in the so-called inertial regime (fast macroscopic deformation), its extended versions have been successfully fitted to observations for a wide range of materials (Kamrin et al. 2024). Thus, it proved versatile, and it is very likely that it can be applied to seasonal sea ice as well (Herman 2022). This has important consequences, because, independently of its particular version, the model has a number of features that are qualitatively different from the other rheological models of sea ice. Crucially, in the viscous-plastic and collisional rheologies, the friction coefficient μ is a constant, whereas in the $\mu(I)$ rheology it is an increasing function of I and thus of the shear rate $\dot{\varepsilon}$.

In general, recent Antarctic observations suggest that the relationship between ice concentration and internal stress is more complex than typically assumed. On the one hand, as

Rheology: studies properties of materials that determine their reaction to deformation and flow, i.e., relationships between external forces acting on a material and its internal reaction (change of shape).

Constitutive equation: (rheological equation of state) relationship between applied forces and geometrical effects induced by them.

Polydispersity: a measure of the heterogeneity of sizes of grains in a granular material

Restitution coefficient: the ratio of the relative velocity of separation after collision to the relative velocity of approach before collision

Inertial number I: nondimensional number relating the macroscopic time scale for bulk deformation to the microscopic time scale for grain rearrangements, computed as $I = \dot{\varepsilon} d/\sqrt{p/\rho}$.

$\mu(I)$ rheology: a rheological model that states that the friction coefficient μ of a material is a function of the inertial number only.

already noted earlier, free drift in the MIZ has been observed at A close to 1 (Womack et al. 2022). On the other hand, decoupling between wind and sea ice motion observed in the MIZ in spring indicates a large role of internal stresses (Womack et al. 2024). This ice-type and season-dependent response to forcing is not yet captured by available rheological models.

4.3. Sea ice melt

3-equation balance: thermodynamics at the ice-ocean interface are fundamentally governed by three equations, which determine 1) the freezing point dependence on salinity and pressure, 2) the conservation of heat, and 3) the conservation of salt.

Sea ice thermodynamic mass loss occurs fundamentally through exchanges with the atmosphere above (e.g., solar heat) or the ocean below. While this mass loss is typically referred to as melting (as we will primarily here), ablation at ice-ocean interfaces technically includes both melting and dissolving. The salinity-dependent freezing temperature and its magnitude relative to the ocean temperature determines the temperature at which mass loss occurs through melting or dissolution (Malyarenko et al. 2020). Melting is predominantly controlled by a heat transfer, which typically occurs when there is a liquid layer of similar salinity to the ice adjacent to the interface (a 'freshwater lens'), while dissolving is controlled by a salt transfer. Dissolution generally occurs when the temperature of the ocean water is less than the freezing temperature of the ice, and the flux of salt towards the ice lowers the freezing point. The typical description of ablation using the '3-equation balance' requires the conservation of heat and salt throughout these processes (Holland & Jenkins 1999). Temporal variability of melt rates is governed by various processes driving the interaction of sea ice with the atmosphere above and the ocean below.

The key to understanding sea ice surface melt is albedo. The albedo (reflectivity) of the sea ice surface determines how much solar energy is absorbed by or transmitted through sea ice versus reflected back to the atmosphere (Perovich & Polashenski 2012). Going into summer, sea ice is typically snow-covered (albedo 0.7-0.9; Light et al. 2022). As Arctic sea ice melts, it can develop a patchwork of bare (white) ice (albedo 0.6-0.7; Smith et al. 2022) and melt ponds (albedo 0.1-0.4; Light et al. 2022). The formation of surface melt ponds on the sea ice plays a large role in increasing the rate of melt by decreasing the albedo. Relatedly, melt ponds can drive a surface melt feedback, where surface melt contributes to expansion and deepening of ponds, which enhances melting. Episodic flushing and drainage of melt ponds often significantly raises the albedo (e.g., Polashenski et al. 2012, Webster et al. 2022). Snow plays a significant role in interannual variability of sea ice surface melt (e.g., Perovich & Richter-Menge 2015), especially as it corresponds to the date of melt initiation or onset (Stroeve et al. 2014).

The dramatically different albedo of dominant surface types drives regional variability in the amount of surface melt. Whereas melt ponds are typically extensive on summer sea ice in the Arctic, resulting in high amounts of surface melt (Perovich & Richter-Menge 2015), Antarctic sea ice has very few ponds and typically thick snow cover, resulting in low ice surface melt (Drinkwater & Liu 2000). The combination of thicker snow and lower relative humidity has led to the general assumption that sea ice surface melt in the Antarctic is negligible, especially as it is typically outpaced by bottom melt.

Melt at the base of sea ice (basal melt) is driven primarily by heat in the ocean below, but the mechanisms by which this heat reaches the bottom of the ice are not always straightforward. During the melt season, relatively cold and fresh meltwater layers can buffer sea ice from warmer and saltier waters in the ocean below (Supply et al. 2022). Thus, basal ablation may actually be dominated by dissolving early in the season (Malyarenko et al. 2020), with melting taking over later in the season after ocean temperatures are warmer and

storms mix up warmer waters from below (e.g., Meyer et al. 2017). Warmer waters can be brought to the surface through wind and wave-induced turbulence (Smith et al. 2018) and small-scale ocean processes. For example, small-scale oceanic currents and surface winds accelerate the basal ice melt rate by allowing warm waters to move into colder regions under the ice floes (Gupta & Thompson 2022), and eddy-induced pumping resulting from friction of the sea ice with the ocean below can pull up warmer waters from below into contact with the ice (Gupta et al. 2020). A key hemispheric difference is that the Southern Ocean has relatively abundant energy for mixing and weak stratification, such that ocean heat can often be more readily accessed for melting throughout the year, including when active growth otherwise dominates in winter (Martinson 1990, e.g.,).

Floes undergo lateral melting at their edges driven by ocean heat in leads or surrounding open water. Waves can cause undercutting (even in relatively small leads; e.g., Richter-Menge et al. 2001) which can further accelerate the erosion of floe edges. The amount of lateral melt is determined by the perimeter of floes exposed to the ocean, which depends on the FSD. Lateral melt is likely a significant contribution to total melt when floe sizes are on the scale of meters (e.g., Bateson et al. 2020). However, as lateral and basal melt generally pull from the same ocean heat reservoir, higher lateral melt near the ice edge may be compensated for by reduced basal ice melt (Tsamados et al. 2015). The distinction is still important to the evolution of the SIZ, as the ice-albedo feedback is most active when ice melts laterally, thereby forming open water (Smith et al. 2022). Vertical melt through surface and basal melt can form open water only once ice is thin, whereas open water can form from lateral melting at any ice thickness.

5. OUTLOOK

Understanding of the processes shaping seasonal sea ice evolution has been developed from a combination of in situ, laboratory and satellite observations, and numerical modeling spanning many spatio-temporal scales (e.g., Fig. 6). In this section, we discuss the knowledge gaps that remain, many of which can be linked to observational or modeling challenges. The SIZ is difficult to observe, due to the difficulty of making field observations from fragmented or weak ice, detecting thin and low concentration sea ice from satellite, characterizing its small-scale heterogeneity, and capturing the episodic nature of storms and waves, amongst other factors. Observational limitations as well as the difficulty in representing the varied processes and sea ice states limit numerical modeling. Below, we summarize some key biases and opportunities associated with improving process-based understanding of seasonal sea ice.

5.1. Biases and missing processes

Observational challenges have led to a seasonal bias, with fall and winter processes associated with sea ice growth (Sec. 4.1) being less well understood than those associated with spring and summer melt and break up. The high-latitude polar oceans are especially challenging for field campaigns to access during polar winter, when ice is thick and storms are powerful. Visible satellite imagery is limited to months with good light, visibility and cloud-free conditions. Biases in sea ice thickness observations from remote sensing, many of which relate to snow and surface properties, complicate our understanding of sea ice congelation growth. The recent development of models for evolution of the sea ice FSD

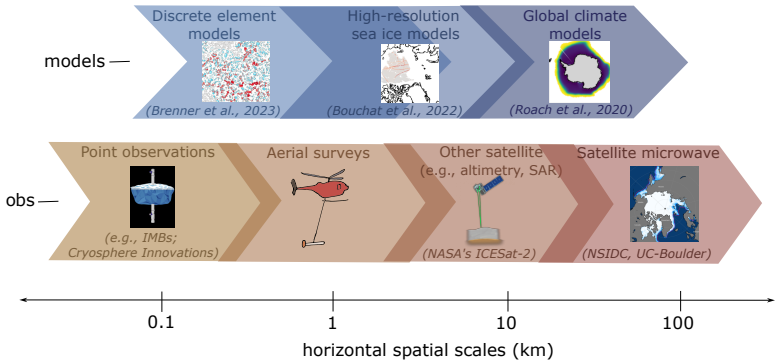

Figure 6: The spatial scales that characterize the modeling (top) and observational tools (bottom) used to understand processes driving seasonal sea ice evolution. Examples shown here include (top) discrete element modeling of floe velocities (Brenner et al. 2023); high resolution modeling of sea ice deformation (Bouchat et al. 2022); global climate modeling of sea ice concentration (Roach et al. 2020); and (bottom) point measurements such as ice mass balance buoys (IMBs), aerial surveys, satellite altimetry, synthetic aperture radar (SAR), and satellite passive microwave observations of sea ice concentration (Meier et al. 2021). Many of the processes discussed herein occur at even smaller scales than are captured by any of the tools shown.

further highlighted seasonal bias: while different methods and theories exist for the fracture of sea ice floes (although this too is far from settled), there is considerable uncertainty on how and to what extent fragmented sea ice heals during freeze-up. Existing schemes are ad-hoc (Bennetts et al. 2017) or based only on geometrical considerations (when sea surface temperatures are below freezing) (Roach et al. 2018a, Boutin et al. 2020). There latter has been tested with field observations (Roach et al. 2018b), but the generality of the welding rate and its sensitivities should be tested further. Field observations also suggest that an existing parametrization for lateral growth (Horvat & Tziperman 2015) may be too conservative (Roach et al. 2018b). These poorly-constrained winter-time processes may have implications for sea ice evolution that impact other seasons.

Our process understanding of seasonal sea ice is notably biased towards the Arctic. Being more accessible to human activity, the Arctic is in general much better observed and understood than the Antarctic; a Google Scholar search shows about 132,000 hits for 'Arctic sea ice' versus 33,000 hits for 'Antarctic sea ice'. Both satellite sea ice observations (e.g., identification of 80 % sea ice concentration contour, Stroeve et al. 2016) and climate models (Roach et al. 2020) have higher skill in the Arctic than the Antarctic, and the Antarctic sees many fewer field campaigns than the Arctic. The Arctic bias is particularly evident for sea ice dynamics; most of the studies cited in Sec. 4.2 are Arctic focused. The existing sea ice rheology models have been developed and tested for the compact Central Arctic ice pack, with the focus on reproducing the characteristic features of ice deformation there (localization and multifractality of deformation, linear kinematic features, and so on). Similarly, satellite products of ice drift and deformation have been more widely tested

against buoy and other *in situ* data in the Northern Hemisphere, and so are likely more reliable there. Few studies consider ice deformation in the Antarctic based on ice drift products (an exception being Tian et al. 2022), and satellite coverage appears lower than in the Arctic (CMEMS 2015), although this is anticipated to improve with upcoming satellite missions. Coverage by autonomous platforms (e.g. ice mass balance buoys and ice-tethered profilers) is poor to non-existent in the Antarctic.

Prior research has been biased towards certain research topics, arguably at the expense of others. For example, the past few decades have seen a strong focus on wave attenuation in sea ice cover. Despite this, the community has not come to consensus on theory (e.g., Thomson 2022, Shen 2022). The disparate approaches to modeling wave attenuation are evident in the variation in attenuation rates (Rogers et al. 2016, Squire 2018) and subsequent impact on the area of sea ice impacted by waves in coupled wave–sea ice modeling (Cooper et al. 2022). Difficulties reconciling observations and models can be attributed to several factors, one of the most important being the fact that different types of information are obtained from the two. Observations, based mostly on satellite data or drifting buoys (e.g., Stopa et al. 2018, Kohout et al. 2020), provide information on the so-called apparent attenuation, i.e., the net change of energy of a given spectral component between two points A and B. In most cases, energy spectra from only two locations are analyzed (or from several buoys analyzed in a pairwise manner), so that the exponential form of the apparent attenuation curves is assumed rather than observed (e.g., Kohout et al. 2020, Alberello et al. 2022). Moreover, the apparent attenuation (Sec. 4.2.2) is influenced by a long list of processes accompanying wave evolution in sea ice: sea ice-related scattering and dissipation (by several different mechanisms within and under the ice), but also wave growth by wind, whitecapping in open water patches, and nonlinear wave–wave interactions. Thus, disentangling from observations the processes directly related to ice – needed for validation of wave-in-ice models – is extremely challenging if not impossible (Rogers et al. 2016). An additional obstacle is the lack or incompleteness of the accompanying data on sea ice properties, including ice type, thickness, and floe size, and their spatio-temporal variability, necessary for attributing the observed attenuation to particular sea ice type and conditions.

In general, many fewer studies have focused on the impact of waves on sea ice than the impact of sea ice on waves. We are beginning to see studies on wave-induced sea ice fracture and wave radiation stress (e.g. Boutin et al. 2020, Voermans et al. 2020), but further research is required. A key challenge is to come up with a model for wave-induced sea ice fracture that does not require the assumptions of total flexion or total rigidity, but tends towards these extreme cases for short and long waves. Establishing a general theory for wave fracture will enable us to better characterize the resulting FSDs, interpret current and future observations, and parametrize this process for large-scale models in a computationally-efficient way. As fracture can rapidly and extensively change the sea ice FSD, exposing the edges of floes to the ocean, it could play an important role in feedback loops (e.g., Asplin et al. 2014).

There are many processes unrelated to waves in the SIZ that are critical to seasonal evolution and deserve further investigation. In terms of thermodynamics, fundamental uncertainties remain in melt and growth rates and how these influence sea ice floe size and thickness. As discussed above, seasonal biases have led to uncertainties in growth rates through the winter. Yet, even melt rates are subject to substantial uncertainties, although they have been relatively well-studied. For example, observational constraints on lateral melt are notably sparse, likely due in part to the locations where it can be expected to

dominate (e.g., SIZ) and the three-dimensional nature of measurements (Richter-Menge et al. 2001). Surface melt is largely driven by the seasonal cycle of albedo, which has been observed to be relatively robust in the Arctic in (Light et al. 2022), but has not been robustly quantified in the Antarctic as the signal is likely dominated by the distribution of snow. In addition, basal growth rates are heavily impacted by the redistribution of snow across sea ice, as snow significantly impacts the vertical heat conduction through the ice and hence the capacity for congelation growth. In the Arctic, the redistribution of snow onto thin ice may impact winter growth rates by up to 8 % (Clemens-Sewall et al. 2022), and large but uncertain losses to leads could have an even larger impact in the Antarctic (Leonard & Maksym 2011). Future work to observe heterogeneity in snow mass balance and to parameterize key processes is needed.

5.2. Connections across scales

In general, connecting the small-scale processes observed during field campaigns to their occurrence and generality throughout the sea ice cover remains difficult. The occurrence and seasonality of different ice types, which would hint at the processes that shaped them, is more or less unknown. Seasonal ice concentration budgets, computed from satellite observations of sea ice concentration and drift, offer information on where sea ice forms and melts at both poles (Holland & Kimura 2016). However, without sea ice thickness observations, such products only offer a two-dimensional view. A large-scale observational characterization of different types of sea ice growth and melt, e.g., a breakdown of sea ice surface, basal and lateral melt, is lacking. This information would advance understanding of seasonal sea ice, and would be especially helpful in validating large-scale climate and sea ice models, many of which now provide these diagnostics.

Large-scale sea ice modeling for climate and earth system models in the past has often taken place separately from research communities with a deep understanding of the relevant processes developed via observations and small-scale, physics-based modeling. As sea ice is tightly coupled to the ocean and atmosphere, it is strongly impacted by biases in either component, and sea ice parameters are often tuned to compensate for climate biases (e.g., Kay et al. 2022). This tuning makes it difficult to quantify to what extent higher sea ice process complexity improves simulation of sea ice and polar climate. The time taken between sea ice parametrization design and testing in a fully-coupled model can be lengthy given model spin-up and ensemble size requirements; simulations without a free-running atmosphere and ocean are computationally cheaper but limit sea ice feedbacks. Simulations that constrain the large-scale atmospheric circulation while preserving coupled sea ice–ocean–atmosphere interactions in the boundary layer could be a promising intermediate path forward (e.g. Pithan et al. 2023). A key challenge for representing small-scale seasonal sea ice processes is to appropriately balance process complexity with model computational expense. In particular, the computational expense of spectral wave models limits advances in modeling wave-ice interactions. As large-scale continuum sea ice models increase in spatial resolution and, in some cases, turn to multi-resolution meshes, it will become increasingly important to explore how oceanic and atmospheric fluxes and dynamics interact with sea ice across spatial scales. Besides horizontal resolution, increases in vertical ocean resolution might have an important influence on sea ice and upper ocean coupling.

Discrete element modeling offers exciting paths forward for developing better understanding of sea ice processes (e.g., Manucharyan & Montemuro 2022, Åström et al. 2023,

Brenner et al. 2023). However, it is key that these efforts are integrated with large-scale modeling approaches to ensure maximal research advances across spatial scales. Future large-scale sea ice models may have DEMs or super-parametrizations embedded within them, or include parametrization informed by DEM modeling. To help bridge the gap, it may be possible to combine DEM and continuum models, e.g., by resolving large floes with a DEM and small floes/grease ice with a continuum model (Marquart et al. 2023). Machine learning has potential to support existing models by replacing expensive parametrizations (Horvat & Roach 2022) or correcting forecasts (Finn et al. 2023). It will be increasingly important to bring together climate modelers and process experts to ensure new modeling technology—whether related to resolution, non-continuum models or machine learning—improves process fidelity.

5.3. Future change

Sea ice zones in both Arctic and Antarctic regions are rapidly changing. The Arctic has been losing multi-year ice for several decades (e.g., Kacimi & Kwok 2022). In 2023 and the early months of 2024, Antarctic sea ice has been anomalously low, with perennial sea ice remaining only in the Weddell Sea (Meier et al. 2021). Wave heights are increasing in both hemispheres as winds intensify (Liu et al. 2024). In the future, a mostly seasonal ice pack may respond differently to atmosphere and ocean forcings, resulting in different feedbacks between thermodynamic and dynamic processes. Some key questions that address future changes in the coupled sea ice system include:

- Will the seasonal cycle of sea ice albedo change with a thinner and more seasonal sea ice pack? Anticipated trends towards thinner ice, lower snowpack, and higher melt pond fractions in both hemispheres would result in lower average albedos. Might this reduce the efficiency of the sea ice albedo feedback?
- How will the partitioning between top, lateral and basal melt change? Basal melt is likely to increase due to anticipated changes in ocean heat content (e.g., Cheng et al. 2022). Lateral melt may also increase from increasingly dynamic forcings and shifts in FSD in both hemispheres. Might this increase the efficiency of the sea ice albedo feedback?
- How will sea ice drift change? As sea surface height increases, summer Arctic sea ice drift may slow down (Ward & Tandon 2023). Will sea ice be less compact on average, and will this impact our understanding of sea ice dynamics?
- As ocean surface waves increase, what role will they play in sea ice feedbacks? In both hemispheres, increasing wave heights might make fragmentation more import and promote formation of pancake ice, which can be a more effective method of sea ice formation. What will the net impact on feedbacks be?
- The connections between sea ice growth and melt and upper ocean heat, salinity and stratification are understood to be important in the Antarctic SIZ (e.g. Wilson et al. 2019) but are poorly observed. They may become more important in the Arctic SIZ with 'Atlantification' under warming (e.g., Asbjørnsen et al. 2020). How will these connections determine future SIZ variability?

As the planet continues to warm, different seasonal sea ice processes have the potential to play an important role in both negative and positive feedback loops. These will have implications for local and global climate, as well direct impacts on hunting and fishing, ecosys-

tems, coastal erosion and native communities. Our community will make most progress by addressing interfaces between subdomains: reconciling observations and modelling, improving process understanding across spatial scales, contrasting the Arctic and Antarctic, and considering the boundaries between different components of the coupled sea ice–ocean–atmosphere system.

DISCLOSURE STATEMENT

The authors are not aware of any affiliations, memberships, funding, or financial holdings that might be perceived as affecting the objectivity of this review.

ACKNOWLEDGMENTS

LR and DR were supported by the NASA Modeling Analysis and Prediction program. AH acknowledges funding from the Polish National Science Centre project no. 2022/47/B/ST10/01129. MMS was supported by Woods Hole Oceanographic Institution Assistant Scientist Endowed Support (ASES). We thank Ted Maksym and Stephen F. Ackley for providing comments that improved the manuscript.

LITERATURE CITED

Alberello A, Bennetts LG, Onorato M, Vichi M, MacHutchon K, et al. 2022. Three-dimensional imaging of waves and floes in the marginal ice zone during a cyclone. *Nature Communications* 13(4590)

Alberello A, Onorato M, Bennetts L, Vichi M, Eayrs C, et al. 2019. Brief communication: Pancake ice floe size distribution during the winter expansion of the Antarctic marginal ice zone. *The Cryosphere* 13(1):41–48

Andreas E, Horst T, Grachev A, Persson P, Fairall C, et al. 2010. Parametrizing turbulent exhange over summer sea ice and the marginal ice zone. *Quart. J. Royal Meteorol. Soc.* 136:927–943

Ardhuin F, Otero M, Merrifield S, Grouazel A, Terrill E. 2020. Ice Breakup Controls Dissipation of Wind Waves Across Southern Ocean Sea Ice. *Geophysical Research Letters* 47(13):e2020GL087699

Asbjørnsen H, Årthun M, Skagseth Ø, Eldevik T. 2020. Mechanisms Underlying Recent Arctic Atlantification. *Geophysical Research Letters* 47(15):e2020GL088036

Asplin MG, Scharien R, Else B, Howell S, Barber DG, et al. 2014. Implications of fractured Arctic perennial ice cover on thermodynamic and dynamic sea ice processes. *Journal of Geophysical Research: Oceans* 119(4):2327–2343

Åström J, Haapala J, Polojärvi A. 2023. A large-scale high-resolution numerical model for sea-ice fragmentation dynamics. *Cryosphere Discussions*

Bateson AW, Feltham DL, Schröder D, Hosekova L, Ridley JK, Aksenov Y. 2020. Impact of sea ice floe size distribution on seasonal fragmentation and melt of Arctic sea ice. *The Cryosphere* 14(2):403–428

Bennetts LG, O'Farrell S, Uotila P. 2017. Brief communication: Impacts of ocean-wave-induced breakup of Antarctic sea ice via thermodynamics in a stand-alone version of the CICE sea-ice model. *The Cryosphere* 11(3):1035–1040

Bouchat A, Hutter N, Chanut J, Dupont F, Dukhovskoy D, et al. 2022. Sea Ice Rheology Experiment (SIREx): 1. Scaling and statistical properties of sea-ice deformation fields. *Journal of Geophysical Research-space Physics* 127:e2021JC017667

Boutin G, Ardhuin F, Dumont D, Sévigny C, Girard-Ardhuin F, Accensi M. 2018. Floe size effect

on wave-ice interactions: Possible effects, implementation in wave model, and evaluation. *Journal of Geophysical Research: Oceans* 123(7):4779–4805

Boutin G, Lique C, Ardhuin F, Rousset C, Talandier C, et al. 2020. Towards a coupled model to investigate wave–sea ice interactions in the Arctic marginal ice zone. *The Cryosphere* 14(2):709–735

Brenner S, Horvat C, Hall P, Lo Piccolo A, Fox-Kemper B, et al. 2023. Scale-dependent air–sea exchange in the polar oceans: Floe–Floe and floe–flow coupling in the generation of ice–ocean boundary layer turbulence. *Geophysical Research Letters* 50:e2023GL105703

Brenner S, Rainville L, Thomson J, Cole S, Lee C. 2021. Comparing Observations and Parameterizations of Ice-Ocean Drag Through an Annual Cycle Across the Beaufort Sea. *Journal of Geophysical Research: Oceans* 126(4):e2020JC016977

Brunette C, Tremblay LB, Newton R. 2022. A new state-dependent parameterization for the free drift of sea ice. *The Cryosphere* 16(2):533–557

Buckley EM, Cañuelas L, Timmermans ML, Wilhelmus MM. 2024. Seasonal Evolution of the Sea Ice Floe Size Distribution from Two Decades of MODIS Data. *EGUsphere* :1–16

Budyko MI. 1969. The effect of solar radiation variations on the climate of the Earth. *Tellus* 21(5):611–619

Cheng L, von Schuckmann K, Abraham JP, Trenberth KE, Mann ME, et al. 2022. Past and future ocean warming. *Nature Reviews Earth & Environment* 3(11):776–794

Clark SP, Doering JC. 2009. Frazil flocculation and secondary nucleation in a counter-rotating flume. *Cold Regions Science and Technology* 55(2):221–229

Clemens-Sewall D, Smith MM, Holland MM, Polashenski C, Perovich D. 2022. Snow redistribution onto young sea ice: Observations and implications for climate models. *Elementa: Science of the Anthropocene* 10(1):00115

CMEMS. 2015. Global Ocean - High Resolution SAR Sea Ice Drift. E.U. Copernicus Marine Service Information.

Cooper VT, Roach LA, Thomson J, Brenner SD, Smith MM, et al. 2022. Wind waves in sea ice of the western Arctic and a global coupled wave-ice model. *Philosophical Transactions of the Royal Society A: Mathematical, Physical and Engineering Sciences* 380(2235):20210258

Daly SF. 1994. International Association for Hydraulic Research Working Group on Thermal Regimes Report on Frazil Ice IAHR AIRH. Tech. rep., US Army Corps of Engineers, Cold Regions Research & Engineering Laboratory

Dansereau V, Weiss J, Saramito P, Lattes P. 2016. A Maxwell elasto-brittle rheology for sea ice modelling. *The Cryosphere* 10(3):1339–1359

Doble MJ. 2009. Simulating pancake and frazil ice growth in the Weddell Sea: A process model from freezing to consolidation. *Journal of Geophysical Research* 114(C9):C09003

Dolatshah A, Bennetts LG, Meylan MH, Monty JP, Toffoli A. 2019. An experimental model of wind-induced rafting of pancake ice floating on waves, In *34th International Workshop on Water Waves and Floating Bodies*, pp. 7–10

Drinkwater MR, Liu X. 2000. Seasonal to interannual variability in Antarctic sea-ice surface melt. *IEEE Transactions on Geoscience and Remote Sensing* 38(4):1827–1842

Dumas-Lefebvre E, Dumont D. 2021. Aerial observations of sea ice break-up by ship waves. *The Cryosphere Discussions* :1–26

Dumont D. 2022. Marginal ice zone dynamics: History, definitions and research perspectives. *Philosophical Transactions of the Royal Society A: Mathematical, Physical and Engineering Sciences* 380(2235):20210253

Dumont D, Kohout A, Bertino L. 2011. A wave-based model for the marginal ice zone including a floe breaking parameterization. *Journal of Geophysical Research* 116(C4):C04001

Feltham DL. 2005. Granular flow in the marginal ice zone. *Philosophical Transactions of the Royal Society A: Mathematical, Physical and Engineering Sciences* 363(1832):1677–1700

Feltham DL. 2008. Sea Ice Rheology. *Annual Review of Fluid Mechanics* 40(1):91–112

Finn T, Durand C, Farchi A, Bocquet M, Chen Y, et al. 2023. Deep learning subgrid-scale parametrisations for short-term forecasting of sea-ice dynamics with a Maxwell elasto-brittle rheology. *The Cryosphere* 17:2965–2991

Gough AJ, Mahoney AR, Langhorne PJ, Williams MJM, Robinson NJ, Haskell TG. 2012. Signatures of supercooling: McMurdo Sound platelet ice. *Journal of Glaciology* 58(207):38–50

Gupta M, Gürcan E, Thompson A. 2024. Eddy-induced dispersion of sea ice floes at the marginal ice zone. *Geophysical Research Letters* 51:e2023GL105656

Gupta M, Marshall J, Song H, Campin JM, Meneghello G. 2020. Sea-Ice Melt Driven by Ice-Ocean Stresses on the Mesoscale. *Journal of Geophysical Research: Oceans* 125(11):e2020JC016404

Gupta M, Thompson AF. 2022. Regimes of Sea-Ice Floe Melt: Ice-Ocean Coupling at the Submesoscales. *Journal of Geophysical Research: Oceans* 127(9):e2022JC018894

Heorton HDBS, Radia N, Feltham DL. 2017. A Model of Sea Ice Formation in Leads and Polynyas. *Journal of Physical Oceanography* 47(7):1701–1718

Herman A. 2011. Molecular-dynamics simulation of clustering processes in sea-ice floes. *Physical Review E* 84(5):056104

Herman A. 2012. Influence of ice concentration and floe-size distribution on cluster formation in sea-ice floes. *Open Physics* 10(3):715–722

Herman A. 2022. Granular effects in sea ice rheology in the marginal ice zone. *Phil. Trans. Royal Soc. A* 380:20210260

Herman A, Dojczman M, Świszcz K. 2020. High-resolution simulations of interactions between surface ocean dynamics and frazil ice. *The Cryosphere* 14(11):3707–3729

Herman A, Wenta M, Cheng S. 2021. Sizes and Shapes of Sea Ice Floes Broken by Waves–A Case Study From the East Antarctic Coast. *Frontiers in Earth Science* 9

Hibler WD. 1979. A dynamic thermodynamic sea ice model. *Journal of Physical Oceanography* 9(4):815–846

Holland DM, Jenkins A. 1999. Modeling Thermodynamic Ice–Ocean Interactions at the Base of an Ice Shelf. *Journal of Physical Oceanography* 29(8):1787–1800

Holland PR, Feltham DL. 2005. Frazil dynamics and precipitation in a water column with depth-dependent supercooling. *Journal of Fluid Mechanics* 530:101–124

Holland PR, Kimura N. 2016. Observed Concentration Budgets of Arctic and Antarctic Sea Ice. *Journal of Climate* 29(14):5241–5249

Horvat C. 2022. Floes, the marginal ice zone and coupled wave-sea-ice feedbacks. *Philosophical Transactions of the Royal Society A: Mathematical, Physical and Engineering Sciences* 380(2235):20210252

Horvat C, Roach LA. 2022. WIFF1.0: A hybrid machine-learning-based parameterization of wave-induced sea ice floe fracture. *Geoscientific Model Development* 15(2):803–814

Horvat C, Roach LLA, Tilling R, Bitz CCM, Fox-Kemper B, et al. 2019. Estimating the sea ice floe size distribution using satellite altimetry: Theory, climatology, and model comparison. *The Cryosphere* 13(11):2869–2885

Horvat C, Tziperman E. 2015. A prognostic model of the sea-ice floe size and thickness distribution. *The Cryosphere* 9(6):2119–2134

Irgens F. 2014. Rheology and non-Newtonian fluids. Springer Int., Switzerland

Jeffries MO, Krouse HR, Hurst-Cushing B, Maksym T. 2001. Snow-ice accretion and snow-cover depletion on Antarctic first-year sea-ice floes. *Annals of Glaciology* 33:51–60

Jop P. 2015. Rheological properties of dense granular flows. *Comptes Rendus Physique* 16:62–72

Jop P, Forterre Y, Pouliquen O. 2006. A constitutive law for dense granular flows. *Nature* 441:727–730

Kacimi S, Kwok R. 2022. Arctic Snow Depth, Ice Thickness, and Volume From ICESat-2 and CryoSat-2: 2018–2021. *Geophysical Research Letters* 49(5):e2021GL097448

Kamrin K, Hill K, Goldman D, Andrade J. 2024. Advances in modeling dense granular media. *Ann. Rev. Fluid Mech.* 56:215–240

Kay JE, DeRepentigny P, Holland M, Bailey D, DuVivier A, et al. 2022. Less surface sea ice melt in the CESM2 improves Arctic sea ice simulation with minimal non-polar climate impacts. *Journal of Advances in Modeling Earth Systems* :doi: 10.1029/2021MS002679

Kohout AL, Smith M, Roach LA, Williams G, Montiel F, Williams MJ. 2020. Observations of exponential wave attenuation in Antarctic sea ice during the PIPERS campaign. *Annals of Glaciology* 61(82):196–209

Kohout AL, Williams MJM, Dean SM, Meylan MH. 2014. Storm-induced sea-ice breakup and the implications for ice extent. *Nature* 509(7502):604–607

Leonard KC, Maksym T. 2011. The importance of wind-blown snow redistribution to snow accumulation on Bellingshausen Sea ice. *Annals of Glaciology* 52(57):271–278

Li H, Lubbad R. 2018. Laboratory study of ice floes collisions under wave action, In *Proc. 28th Int. Ocean and Polar Engng Conf. ISOPE-2018*

Light B, Smith M, Perovich D, Webster M, Holland M, et al. 2022. Arctic sea ice albedo: Spectral composition, spatial heterogeneity, and temporal evolution observed during the MOSAiC drift. *Elementa Science of the Anthropocene*

Liu J, Li R, Li S, Meucci A, Young IR. 2024. Increasing wave power due to global climate change and intensification of Antarctic Oscillation. *Applied Energy* 358:122572

Longuet-Higgins MS, w. Stewart R. 1964. Radiation stresses in water waves; a physical discussion, with applications. *Deep Sea Research and Oceanographic Abstracts* 11(4):529–562

Lu P, Li Z, Cheng B, Leppäranta M. 2011. A parameterization of the ice-ocean drag coefficient. *Journal of Geophysical Research* 116(C7):C07019

Maksym T. 2019. Arctic and Antarctic Sea Ice Change: Contrasts, Commonalities, and Causes. *Annual Review of Marine Science* 11(1):187–213

Malyarenko A, Wells AJ, Langhorne PJ, Robinson NJ, Williams MJ, Nicholls KW. 2020. A synthesis of thermodynamic ablation at ice-ocean interfaces from theory, observations and models. *Ocean Modelling* :101692

Manucharyan GE, Montemuro BP. 2022. SubZero: A Sea Ice Model With an Explicit Representation of the Floe Life Cycle. *Journal of Advances in Modeling Earth Systems* 14(12):e2022MS003247

Manucharyan GE, Thompson AF. 2017. Submesoscale Sea Ice-Ocean Interactions in Marginal Ice Zones. *Journal of Geophysical Research: Oceans* 122(12):9455–9475

Marquart R, Bogaers A, Skatulla S, Alberello A, Toffoli A, Schwarz C. 2023. Small-scale computational fluid dynamics modelling of the wave induced ice floe-grease ice interaction in the Antarctic marginal ice zone. *Cold Regions Science and Technology* :104108

Martinson DG. 1990. Evolution of the southern ocean winter mixed layer and sea ice: Open ocean deepwater formation and ventilation. *Journal of Geophysical Research* 95(C7):11641

McFarlane V, Loewen M, Hicks F. 2014. Laboratory measurements of the rise velocity of frazil ice particles. *Cold Regions Sci. Tech.* 106–107:120–130

Mchedlishvili A, Lüpkes C, Petty A, Tsamados M, Spreen G. 2023. New estimates of pan-Arctic sea ice–atmosphere neutral drag coefficients from ICESat-2 elevation data. *The Cryosphere* 17:4103–4131

Meier W, Fetterer F, Windnagel A, Stewart S. 2021. NOAA/NSIDC Climate Data Record of Passive Microwave Sea Ice Concentration, Version 4

Meyer A, Fer I, Sundfjord A, Peterson AK. 2017. Mixing rates and vertical heat fluxes north of Svalbard from Arctic winter to spring. *Journal of Geophysical Research: Oceans* 122(6):4569–4586

Mokus NGA, Montiel F. 2022. Wave-triggered breakup in the marginal ice zone generates lognormal floe size distributions: A simulation study. *The Cryosphere* 16(10):4447–4472

Morse B, Richard M. 2009. A field study of suspended frazil ice particles. *Cold Regions Science and Technology* 55(1):86–102

Nakata K, Ohshima K, Nihashi S. 2021. Mapping of active frazil for Antarctic coastal polynyas, with an estimation of sea-ice production. *Geophysical Research Letters* 48:e2020GL091353

Naumann AK, Notz D, Håvik L, Sirevaag A. 2012. Laboratory study of initial sea-ice growth: Properties of grease ice and nilas. *The Cryosphere* 6(4):729–741

Nose T, Waseda T, Kodaira T, Inoue J. 2020. On the coagulated pancake ice formation: Observation in the refreezing Chukchi Sea and comparison to the Antarctic consolidated pancake ice. *Polar Science* :100622

Ólason E, Boutin G, Korosov A, Rampal P, Williams T, et al. 2022. A New Brittle Rheology and Numerical Framework for Large-Scale Sea-Ice Models. *Journal of Advances in Modeling Earth Systems* 14(8):e2021MS002685

Perovich DK, Polashenski C. 2012. Albedo evolution of seasonal Arctic sea ice. *Geophysical Research Letters* 39(8):n/a–n/a

Perovich DK, Richter-Menge JA. 2015. Regional variability in sea ice melt in a changing Arctic. *Philosophical Transactions of the Royal Society A: Mathematical, Physical and Engineering Sciences* 373(2045):20140165

Pithan F, Athanase M, Dahlke S, Sánchez-Benítez A, Shupe MD, et al. 2023. Nudging allows direct evaluation of coupled climate models with in situ observations: A case study from the MOSAiC expedition. *Geoscientific Model Development* 16(7):1857–1873

Polashenski C, Perovich D, Courville Z. 2012. The mechanisms of sea ice melt pond formation and evolution. *Journal of Geophysical Research: Oceans* 117(C1)

Prinsenberg SJ, Peterson IK. 2011. Observing regional-scale pack-ice decay processes with helicopter-borne sensors and moored upward-looking sonars. *Annals of Glaciology* 52(57):35–42

Rees Jones DW, Wells AJ. 2015. Solidification of a disk-shaped crystal from a weakly supercooled binary melt. *Physical Review E* 92(2):022406

Rees Jones DW, Wells AJ. 2018. Frazil-ice growth rate and dynamics in mixed layers and sub-ice-shelf plumes. *The Cryosphere* 12(1):25–38

Richter-Menge JA, Perovich DK, Pegau WS. 2001. Summer ice dynamics during SHEBA and its effect on the ocean heat content. *Annals of Glaciology* 33:201–206

Roach LA, Dörr J, Holmes CR, Massonnet F, Blockley EW, et al. 2020. Antarctic sea ice area in CMIP6. *Geophysical Research Letters* 47(9):1–10

Roach LA, Eisenman I, Wagner TJW, Blanchard-Wrigglesworth E, Bitz CM. 2022. Asymmetry in the seasonal cycle of Antarctic sea ice driven by insolation. *Nature Geoscience* 15(4):277–281

Roach LA, Horvat C, Dean SM, Bitz CM. 2018a. An emergent sea ice floe size distribution in a global coupled ocean–sea ice model. *Journal of Geophysical Research: Oceans* 123(6):4322–4337

Roach LA, Smith MM, Dean SM. 2018b. Quantifying growth of pancake sea ice floes using images from drifting buoys. *Journal of Geophysical Research: Oceans* 123(4):2851–2866

Rogers WE, Thomson J, Shen HH, Doble MJ, Wadhams P, Cheng S. 2016. Dissipation of wind waves by pancake and frazil ice in the autumn Beaufort Sea. *Journal of Geophysical Research: Oceans* 121(11):7991–8007

Roquet F, Ferreira D, Caneill R, Schlesinger D, Madec G. 2022. Unique thermal expansion properties of water key to the formation of sea ice on Earth. *Science Advances* 8(46):eabq0793

Rothrock DA, Thorndike AS. 1984. Measuring the sea ice floe size distribution. *Journal of Geophysical Research* 89(C4):6477

Rynders S, Aksenov Y, Feltham D, Nurser A, Madec G. 2022. Impact of granular behaviour of fragmented sea ice on marginal ice zone dynamics, In *IUTAM Symposium on Physics and Mechanics of Sea Ice*, eds. J Tuhkuri, A Polojärvi, no. 39 in IUTAM Bookseries, pp. 261–274, Springer Nature Switzerland

Schneck CC, Ghobrial TR, Loewen MR. 2019. Laboratory study of the properties of frazil ice particles and flocs in water of different salinities. *The Cryosphere* 13(10):2751–2769

Shen H, Hibler III W, Leppäranta M. 1984. On the rheology of a broken ice field due to floe collision. *MIZEX Bulletin III, USACREL Special Report 84-28* :29–34

Shen HH. 2022. Wave-in-ice: Theoretical bases and field observations. *Philosophical Transactions of the Royal Society A: Mathematical, Physical and Engineering Sciences* 380(2235):20210254

Shen HH, Ackley SF, Hopkins MA. 2001. A conceptual model for pancake-ice formation in a wave field. *Annals of Glaciology* 33(2):361–367

Shen HH, Hibler WD, Lepparanta M. 1986. On applying granular flow theory to a deforming broken ice field. *Acta Mechanica* 63(1-4):143–160

Shen HH, Hibler WD, Leppäranta M. 1987. The role of floe collisions in sea ice rheology. *Journal of Geophysical Research* 92(C7):7085

Shen HH, Sankaran B. 2004. Internal length and time scales in a simple shear granular flow. *Physical Review E* 70(5):051308

Smedsrud LH. 2011. Grease-ice thickness parameterization. *Annals of Glaciology* 52(57):77–82

Smedsrud LH, Martin T. 2015. Grease ice in basin-scale sea-ice ocean models. *Annals of Glaciology* 56(69):295–306

Smith M, Stammerjohn S, Persson O, Rainville L, Liu G, et al. 2018. Episodic Reversal of Autumn Ice Advance Caused by Release of Ocean Heat in the Beaufort Sea. *Journal of Geophysical Research: Oceans* 123(5):3164–3185

Smith M, Thomson J. 2020. Pancake sea ice kinematics and dynamics using shipboard stereo video. *Annals of Glaciology* 61(82):1–11

Smith MM, Holland M, Light B. 2022. Arctic sea ice sensitivity to lateral melting representation in a coupled climate model. *The Cryosphere* 16(2):419–434

Squire VA. 2018. A fresh look at how ocean waves and sea ice interact. *Philosophical Transactions of the Royal Society A: Mathematical, Physical and Engineering Sciences* 376(2129):20170342

Stern HL, Schweiger AJ, Stark M, Zhang J, Steele M, Hwang B. 2018. Seasonal evolution of the sea-ice floe size distribution in the Beaufort and Chukchi seas. *Elementa: Science of the Anthropocene* 6(1):48

Stopa JE, Sutherland P, Ardhuin F. 2018. Strong and highly variable push of ocean waves on Southern Ocean sea ice. *Proceedings of the National Academy of Sciences* 115(23):5861–5865

Stroeve JC, Jenouvrier S, Campbell GG, Barbraud C, Delord K. 2016. Mapping and assessing variability in the Antarctic marginal ice zone, pack ice and coastal polynyas in two sea ice algorithms with implications on breeding success of snow petrels. *The Cryosphere* 10(4):1823–1843

Stroeve JC, Markus T, Boisvert L, Miller J, Barrett A. 2014. Changes in Arctic melt season and implications for sea ice loss. *Geophysical Research Letters* 41(4):1216–1225

Sumata H, de Steur L, Divine DV, Granskog MA, Gerland S. 2023. Regime shift in Arctic Ocean sea ice thickness. *Nature* 615(7952):443–449

Supply A, Boutin J, Kolodziejczyk N, Reverdin G, Lique C, et al. 2022. Meltwater lenses over the Chukchi and the Beaufort seas during summer 2019: From in situ to synoptic view. *Journal of Geophysical Research: Oceans* 127(12):e2021JC018388

Sutherland P, Dumont D. 2018. Marginal Ice Zone Thickness and Extent due to Wave Radiation Stress. *Journal of Physical Oceanography* 48(8):1885–1901

Thomson J. 2022. Wave propagation in the marginal ice zone: Connections and feedback mechanisms within the air–ice–ocean system. *Philosophical Transactions of the Royal Society A: Mathematical, Physical and Engineering Sciences* 380(2235):20210251

Thorndike AS, Rothrock DA, Maykut GA, Colony R. 1975. The thickness distribution of sea ice. *Journal of Geophysical Research* 80(33):4501–4513

Tian TR, Fraser AD, Kimura N, Zhao C, Heil P. 2022. Rectification and validation of a daily satellite-derived Antarctic sea ice velocity product. *The Cryosphere* 16(4):1299–1314

Timmermann R. 2004. Utilizing the ASPeCt sea ice thickness data set to evaluate a global coupled sea ice–ocean model. *Journal of Geophysical Research* 109(C7):C07017

Toyota T, Haas C, Tamura T. 2011. Size distribution and shape properties of relatively small sea-ice floes in the Antarctic marginal ice zone in late winter. *Deep Sea Research Part II: Topical Studies in Oceanography* 58(9-10):1182–1193

Tsamados M, Feltham D, Petty A, Schroeder D, Flocco D. 2015. Processes controlling surface, bot-

tom and lateral melt of Arctic sea ice in a state of the art sea ice model. *Philosophical Transactions of the Royal Society A: Mathematical, Physical and Engineering Sciences* 373(2052):20140167

Tsamados M, Feltham DL, Schroeder D, Flocco D, Farrell SL, et al. 2014. Impact of variable atmospheric and oceanic form drag on simulations of Arctic sea ice. *Journal of Physical Oceanography* 44(5):1329–1353

Vichi M. 2022. An indicator of sea ice variability for the Antarctic marginal ice zone. *The Cryosphere* 16(10):4087–4106

Voermans JJ, Babanin AV, Thomson J, Smith MM, Shen HH. 2019. Wave attenuation by sea ice turbulence. *Geophysical Research Letters*

Voermans JJ, Rabault J, Filchuk K, Ryzhov I, Heil P, et al. 2020. Experimental evidence for a universal threshold characterizing wave-induced sea ice break-up. *The Cryosphere* 14(11):4265–4278

Wagner TJW, Eisenman I. 2015. How Climate Model Complexity Influences Sea Ice Stability. *Journal of Climate* 28(10):3998–4014

Wagner TJW, Eisenman I, Ceroli AM, Constantinou NC. 2022. How Winds and Ocean Currents Influence the Drift of Floating Objects. *Journal of Physical Oceanography* 52(5):907–916

Wahlgren S, Thomson J, Biddle LC, Swart S. 2023. Direct Observations of Wave-Sea Ice Interactions in the Antarctic Marginal Ice Zone. *Journal of Geophysical Research: Oceans* 128(10):e2023JC019948

Wakatsuchi M, Ono N. 1983. Measurements of salinity and volume of brine excluded from growing sea ice. *Journal of Geophysical Research: Oceans* 88(C5):2943–2951

Ward JL, Tandon NF. 2023. Why is Summertime Arctic Sea Ice Drift Speed Projected to Decrease? *The Cryosphere Discussions* :1–29

Webster MA, Holland M, Wright NC, Hendricks S, Hutter N, et al. 2022. Spatiotemporal evolution of melt ponds on Arctic sea ice: MOSAiC observations and model results. *Elem Sci Anth* 10(1):000072

Wells AJ, Hitchen JR, Parkinson JRG. 2019. Mushy-layer growth and convection, with application to sea ice. *Philosophical Transactions of the Royal Society A: Mathematical, Physical and Engineering Sciences* 377(2146):20180165

Williams TD, Bennetts LG, Squire VA, Dumont D, Bertino L. 2013. Wave–ice interactions in the marginal ice zone. Part 2: Numerical implementation and sensitivity studies along 1D transects of the ocean surface. *Ocean Modelling* 71:92–101

Wilson EA, Riser SC, Campbell EC, Wong APS. 2019. Winter Upper-Ocean Stability and Ice–Ocean Feedbacks in the Sea Ice–Covered Southern Ocean. *Journal of Physical Oceanography* 49(4):1099–1117

Womack A, Alberello A, de Vos M, Toffoli A, Verrinder R, Vichi M. 2024. A contrast in sea ice drift and deformation between winter and spring of 2019 in the Antarctic marginal ice zone7. *The Cryosphere* 18:205–229

Womack A, Vichi M, Alberello A, Toffoli A. 2022. Atmospheric drivers of a winter-to-spring Lagrangian sea-ice drift in the Eastern Antarctic marginal ice zone. *J. Glaciology* 68:999–1013

Worby AP, Geiger CA, Paget MJ, Van Woert ML, Ackley SF, DeLiberty TL. 2008. Thickness distribution of Antarctic sea ice. *Journal of Geophysical Research* 113(C5):C05S92

Yulmetov R, Lubbad R, Løset S. 2016. Planar multi-body model of iceberg free drift and towing in broken ice. *Cold Regions Sci. Technol.* 121:154–166

Zhaka V, Bridges R, Riska K, Hagermann A, Cwirzen A. 2023. Initial snow-ice formation on a laboratory scale. *Annals of Glaciology* :1–18